Adsorption of Quantum Dots onto Polymer and Gemini Surfactant Films: A Quartz Crystal Microbalance Study

ARTICLE *in* LANGMUIR · AUGUST 2014

Impact Factor: 4.46 · DOI: 10.1021/la5024955 · Source: PubMed

3 AUTHORS:

Teresa Alejo

University of Zaragoza

4 PUBLICATIONS **16** CITATIONS

SEE PROFILE

María Dolores Merchán Moreno

Universidad de Salamanca

20 PUBLICATIONS **152** CITATIONS

SEE PROFILE

Maria Mercedes Velázquez

Universidad de Salamanca

60 PUBLICATIONS **608** CITATIONS

SEE PROFILE

Langmuir

Article

pubs.acs.org/Langmuir

Adsorption of Quantum Dots onto Polymer and Gemini Surfactant Films: A Quartz Crystal Microbalance Study

T. Alejo, M. D. Merchán, and M. M. Velázquez*

Departamento de Química Física, Facultad de Ciencias Químicas, Universidad de Salamanca. 37008 Salamanca, Spain

Supporting Information

ABSTRACT: We used quartz crystal microbalance with dissipation to study the mechanical properties, the kinetics of adsorption, and the amount of CdSe quantum dots (QDs) adsorbed onto a SiO_2 sensor, referred as bare sensor, onto the sensor modified with a film of the polymer poly(maleic anhydride-*alt*-1-octadecene), PMAO, or with a film of the Gemini surfactant ethyl-bis(dimethyl octadecyl ammonium bromide), abbreviated as 18-2-18. Results showed that when the sensor is coated with polymer or surfactant molecules, the coverage increases compared with that obtained for the bare sensor. On the other hand, rheological properties and kinetics of adsorption of QDs are driven by QD nanoparticles. Thus, the QD films present elastic behavior, and the elasticity values are independent of the molecule used as coating and similar to the elasticity value obtained for QDs films on the bare sensor. The QD adsorption is a two-step mechanism in which the fastest process is attributed to the QD adsorption onto the solid substrate and the slowest one is ascribed to rearrangement movements of the nanoparticles adsorbed at the surface.

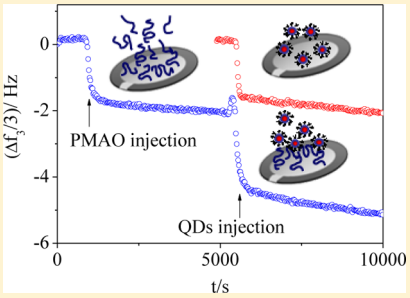

1. INTRODUCTION

Semiconductor nanocrystal CdSe quantum dots (QDs) are widely used in optoelectronic devices such as light emitting diodes (LEDs), solar cells, or nanosensors due to their unique optical properties.[1−5] For construction of nanostructured devices with QDs, it is necessary to support them on solid substrates.[2,6] In these cases, the organization of nanoparticles into ordered arrays can lead to new interesting properties, which are strongly affected by the morphology of the nanoparticle film.[7−10] One important problem to be resolved in these situations is the nanoparticle agglomeration because it decreases the quality of the devices.[11,12] The most recent efforts involve the use of polymer or surfactant molecules to minimize nanoparticles 3D aggregation. Despite the great interest generated in recent years on this topic, more work must be carried out to develop multifunctional materials with novel electric, magnetic, or optical properties.[13] With this objective in mind, in previous work, we have carried out a systematic study of the effect of coating molecules such as the copolymers, poly(maleic anhydride-*alt*-1-octadecene), PMAO, and poly(styrene-*co*-maleic anhydride) partial 2 buthoxy ethyl ester cumene terminated, PS-MA-BEE, and the Gemini surfactant, ethyl-bis(dimethyl octadecyl ammonium bromide), abbreviated as 18-2-18, on the self-assembly process of semiconductor crystal of CdSe QDs at the interface.[14−18] In this previous work, the QD films were prepared by the Langmuir−Blodgett (LB) methodology because it allows the continuous variation of particle density, spacing, and arrangement by compressing or expanding the film using barriers.[19] Consequently, it offers the possibility of preparing reproducible films of polymers, surfactants, and nanoparticles with the control of interparticle distance necessary to exploit the nanocomposites in technological applications.[20,21] We have chosen these molecules as coatings because they anchor to solid substrates such as mica or silicon through their hydrophilic moieties and to the nanoparticles by attractive interactions between their hydrophobic parts and the QD stabilizer trioctylphosphine oxide (TOPO). In addition, it is well established that the polymer PMAO avoids the three-dimensional (3D) aggregation of some nanoparticles[22−25] and PMAO-capped nanoparticles have been successfully incorporated onto solid substrates by the LB technique.[26] On the other hand, the Gemini surfactant 18-2-18 combined with DNA was proposed for biotechnological applications.[27,28]

In previous work, we analyzed the effect of different factors such as the methodology of film deposition, the surface density, and the shear stress on the morphology of the QD LB films. Our results demonstrated that the morphology of QD domains strongly depends of these factors.[14−18] Moreover, the intensity and lifetime of fluorescence emission is influenced by the morphology of QD domains.[17] This is an important issue because CdSe QDs have been proposed as components for fabrication of LEDs.[2,29,30] An interesting result obtained in our previous work was that both the polymer PMAO and the surfactant 18-2-18 avoid the 3D aggregation of QDs,[14−18] and that the most packed and ordered QD domains correspond to films of nanoparticles adsorbed on LB films of the Gemini surfactant.[14] On the other hand, atomic force microscopy (AFM) and scanning electron microscopy (SEM) images of QD films onto the coated sensor were taken several months

Received: March 13, 2014
Revised: July 30, 2014
Published: August 5, 2014

   dx.doi.org/10.1021/la5024955 | *Langmuir* 2014, 30, 9977−9984

after preparation and showed no differences compared with fresh films. This means that these QD films have long term stability against 3D aggregation. This is an important issue for potential applications of QDs.

Once the effect of the methodology of deposition and the surface density on the morphology of QD films is analyzed, it becomes necessary to study the influence of coatings on the QD coverage and to determine the kinetics properties of the adsorption process and the rheological properties of films. All this information is critical to understand the role of the coating molecules on the morphology and properties of QD films to improve the properties of films used as component of optoelectronic devices. Since quartz crystal microbalance with dissipation (QCM-D) allows monitoring in situ the mass adsorbed, the adsorption kinetics, and the conformational changes of molecules adsorbed on solids,[31−33] we use this technique to investigate the kinetics of the adsorption process, the rheological properties of QD films, and the coverage of coated and bare sensors.

2. MATERIALS AND METHODS

2.1. Materials. The polymer poly(maleic anhydride-*alt*-1-octadecene), PMAO (M_r = 40 kDa), was purchased from Sigma-Aldrich. The Gemini surfactant ethyl-bis(dimethyl octadecyl ammonium bromide), abbreviated as 18-2-18, was synthesized using the method described by Zana et al.[34] with some modifications in the crystallization step.[35]

The synthesis of CdSe QDs capped with trioctylphosphine oxide (TOPO) was carried out by the method proposed by Yu and Peng.[36] The QDs' size (diameter 3.55 ± 0.05 nm) and concentration were determined by the position and intensity of the maximum of the visible spectrum of the QDs dispersed in chloroform.[37] UV−vis absorption spectra were recorded on the Shimadzu UV-2401PC spectrometer.

Chloroform (PAI, filtered) used to prepare the solutions was from Sigma-Aldrich. The solution concentrations ranged from 5×10^{-7} to 1×10^{-2} M. The quartz sensor crystals coated with silicon oxide (QSX 303) were supplied by Q-Sense.

2.2. Quartz Crystal Microbalance with Dissipation (QCM-D). The QCM experiments were performed on the QCM-D model Q-Sense E1 (Gothenburg, Sweden). The quartz sensor crystals used consist of an AT-cut quartz crystal of 14 mm of diameter and thickness 0.3 mm coated with SiO_2. The cleaning procedure for the sensors was done by sonication in chloroform (15 min) and after that washing with acetone (PAI quality 99%, Panreac), ultrapure water and ethanol (PAI quality 99.5%, Panreac) and finally dried with air/nitrogen flow. The ultrapure water was prepared by a combination of RiOs and Milli-Q systems from Millipore.

The crystal is excited to oscillate at its characteristic fundamental frequency f_0 = 5 MHz and its odds overtones (ν = 3, 5, 7, 9 and 11). The adsorption of mass on the crystal surface is registered as a decrease in the resonance frequency (Δf), while changes in the dissipation factor (ΔD) are related to the viscoelastic properties and to structural changes of the film.

The methodology employed for the adsorption of the successive layers in the QCM-D experiments was the following: to set the baseline, the solvent used for preparing the solutions, chloroform, was introduced in the measurement chamber cell using a peristaltic pump at the flow rate of 50 μL min^{-1}. In a second stage, the polymer or surfactant solution (ranged from 5×10^{-4} to 1×10^{-2} M) was introduced in the cell at the same flow rate until it was fully filled. Then, the flow was stopped and the experiments were performed in batch conditions at 20 °C. After covering the sensor with the surfactant or polymer coating molecules, the QDs were deposited onto the first layer by filling the cell with the QD solution in chloroform (ranged from 5×10^{-7} to 8×10^{-6} M). For elastic films,[38] the Sauerbrey relationship, $\Delta m = -(C\Delta F)/\nu$, can be used to calculate the mass deposited onto the crystal.[39] In the Sauerbrey equation, the parameter C represents the mass sensitivity constant (17.7 Hz^{-1} ng cm^{-2} at 5 MHz) and ν is the overtone used in the calculation. When the contribution of the layer viscosity to the dissipation factor it is not negligible, the Voigt model for viscoelastic films is used to determine the mass adsorbed, thickness, and rheological parameters.[40] We use this model implemented in the software of Q-Sense equipment (Qtools modeling software) for the polymer films; see below.

3. RESULTS AND DISCUSSION

3.1. Properties of Polymer and Gemini Surfactant Films. Prior to study the effect of polymer and surfactant coatings on the properties of QDs films, it was necessary to characterize the coating films. Two typical records obtained by QCM-D at five frequency overtones (ν = 3, 5, 7, 9, 11) as a function of time are shown in Figure 1a,b for PMAO and Gemini surfactant films, respectively. The first stage observed in the curves corresponds to the baseline obtained by introducing the solvent, chloroform, in the cell. A sharp decrease in the frequency shift, associated with the adsorption of coating molecules on the sensor surface, is observed when the coating solution is introduced in the cell. The end of the adsorption process was taken when $\Delta f/\nu$ reached a constant value; see Figure 1a,b. Experimental $\Delta f/\nu$ and ΔD data in Figure 1 point out to different rheological properties. Thus, for PMAO films,

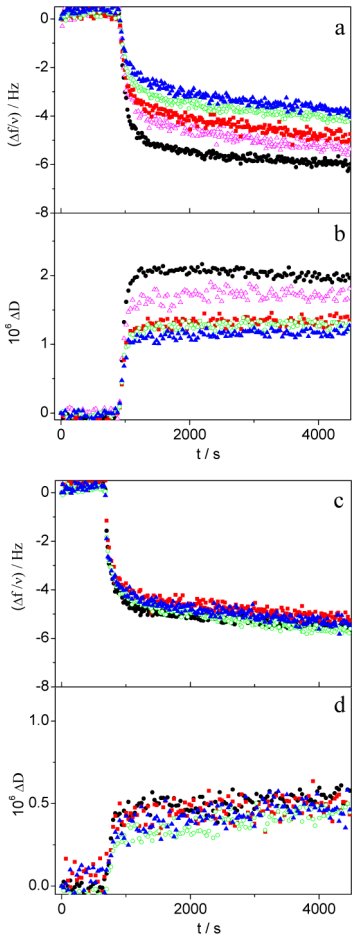

Figure 1. Time dependence of the $\Delta f/\nu$ and ΔD shifts for different frequency overtones, 3rd (black), 5th (pink), 7th (red), 9th (green), and 11th (blue), during the absorption of (a, b) the PMAO layer (concentration of the polymer solution in cell 1×10^{-2} M) and (c, d) the Gemini surfactant (concentration of the surfactant solution in cell 1×10^{-3} M).

dx.doi.org/10.1021/la5024955 | Langmuir 2014, 30, 9977−9984

Δf does not overlap for the different overtones and changes in ΔD are high with respect to changes in frequency. We calculated the $\Delta D/\Delta f$ values for the polymer films, and they vary from 9% to 25% depending on the polymer concentration and the overtone considered. These values are higher than 5%, indicating that the added mass acts as a soft and dissipative adlayer. In this situation, the Voigt viscoelastic model is typically used to interpret the QCM-D results.[41,42] Briefly, the model describes viscoelastic behavior in films on the basis of two components, the elastic component interpreted as a spring and the viscous contribution interpreted as a dashpot. Accordingly, the viscoelastic adlayer is characterized by the complex shear modulus, G^*, as follows:

$$G^* = G' + iG'' = \mu_1 + i2\pi f\eta_1 \quad (1)$$

where G' and, G'' represent the storage and loss modulus, respectively. μ_1 is the elastic shear modulus, f is the oscillation frequency, and η_1 is the shear viscosity. In contrast, results corresponding to the Gemini surfactant films (Figure 1c,d) showed that changes in frequency and dissipation converge in master curves for the different overtones. This means that the surfactant films can be considered rigid.[42] Accordingly, the mass adsorbed for Gemini surfactant films is calculated by the Sauerbrey equation using the 3rd, 5th, 7th, 9th, and 11th overtones and the values are independent of the overtone used for calculations, as expected from elastic films.

According to these results, the Voigt model was used to interpret the QCM-D data of the polymer PMAO. The model involves four parameters of the adlayer,[38] the thickness, density, viscosity, and shear modulus, and it considers that the viscoelastic adlayer is in contact with bulk Newtonian fluid, chloroform in our system. The fitting of the experimental data to the Voigt model was done by minimizing the chi-square value (χ^2) to give the best-fit values by means of the Q-Tools software. According to the model, the Δf and ΔD values are related to the liquid and adlayer parameters by eqs 2 and 3 of the Supporting Information. Details of the fitting procedure, along with the boundary conditions, are disclosed in the section 1 of the Supporting Information. The fits for all PMAO films are in good agreement with experimental data; see Figure 1s of the Supporting Information.

Figure 2a shows the G' and G'' values calculated with the best fitting parameters and eq 1 against the PMAO concentration. The G'' values are calculated from eq 2 with f = 5 MHz. Results showed that both G' and G'' values are almost independent of polymer concentration and the average values found were 0.4 and 0.04 MPa for G' and G'', respectively. Since the G' is higher than G'', the film is predominantly rigid; however, the G'/G'' ratio is not too high, indicating that the viscous contribution is not negligible and has to be take into account to properly interpret the rheological properties of the polymer films.

Differences observed between the rheological properties of the polymer PMAO and the Gemini surfactant films can be related to the structure of molecules adsorbed on the sensor.[43] It is well established that an easy way to visualize differences[43] is to analyze the variation of ΔD against $\Delta f_\nu/\nu$. Therefore, to gain insights into the structure of these films, we plot ΔD vs $\Delta f_3/3$ in Figure 2b. We have represented results corresponding to the third overtone (15 MHz) because it was proved to be the most consistent and offers higher signal-to-noise ratio.[44] Data presented in Figure 2b show two different trends. Thus, the slope of the dissipation change (ΔD_3) against $\Delta f_3/3$ is higher

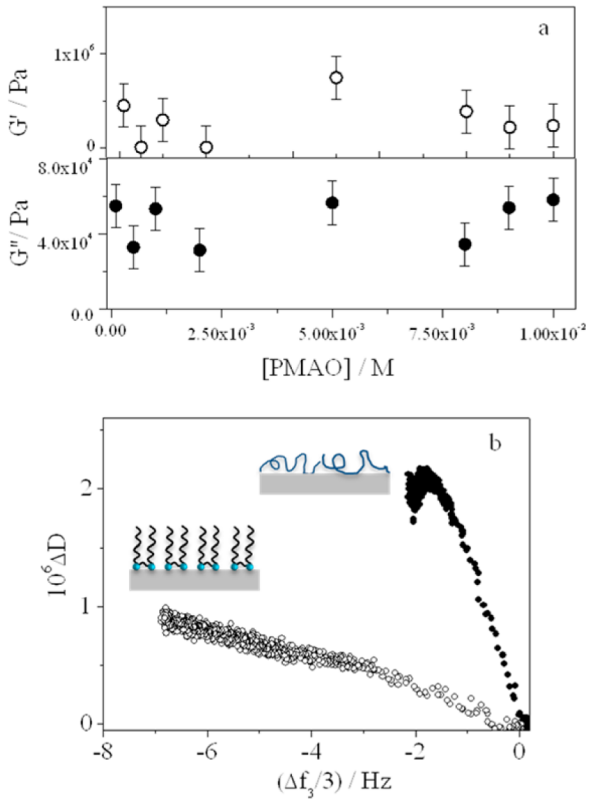

Figure 2. (a) Variation of G' (open symbols) and G'' (solid symbols) values with the PMAO concentration of solutions in the cell. (b) ΔD vs $\Delta f/\nu$ plots for (solid symbols) PMAO film (concentration of the polymer solution in cell 1×10^{-2} M) and (open symbols) Gemini surfactant film (concentration of the surfactant solution in cell 1×10^{-3} M).

for PMAO films than for Gemini ones. This fact suggests flatter conformation for PMAO than for the surfactant film likely due to higher molecular packing on Gemini films than on polymer ones. The higher packing of the surfactant molecules can be responsible of the elastic behavior found in this film.[43] To confirm this assumption, the film thickness was calculated from QCM-D measurements and the values found are collected in Table 1. For comparison, Table 1 also presents the height

Table 1. K_L and Γ_{max} Values Obtained for the Fitting of the Absorption Data to the Langmuir Equation and Thickness Obtained for the Layers Using QCM and AFM

	thickness/nm			
coating	QCM	AFM	$K_L/(\text{mol L})^{-1}$	$\Gamma_{max}/\text{mol m}^{-2}$
PMAO	2.0 ± 1.0	1.5 ± 0.2[a]	$(6 \pm 0.5) \times 10^3$	1.1×10^{-7}
Gemini	2.3 ± 0.5	2.0 ± 0.5[b]	$(20 \pm 0.5) \times 10^3$	21×10^{-7}

[a]Reference 10. [b]References 13 and 33.

profiles determined from AFM measurements for films deposited on mica by the Langmuir–Blodgett methodology.[14,35] From data in Table 1, it is possible to conclude that the thickness values obtained by QCM-D are in good agreement with the average height profiles of LB films determined by AFM. Moreover, the thickness of the surfactant layer is close to the length of a fully extended hydrocarbon chain of 18C atoms (2.4 nm)[14,35] while the thickness obtained for PMAO films are smaller. Taking into account that both

dx.doi.org/10.1021/la5024955 | Langmuir 2014, 30, 9977−9984

molecules contain hydrocarbon chains of 18C atoms, our results indicate that the surfactant molecules adopt a configuration almost perpendicular to the solid surface while the polymer molecules are tilted, resulting in a flat configuration at the interface. This is consistent with the qualitative information reported above from the ΔD and Δf values.

From Figure 2b, we get qualitative information about the enthalpy/entropy balance of the adsorption process.[45,46] The high dissipation factor values ($\Delta D \sim 2 \times 10^{-6}$) found for the PMAO films can be associated with a low weight of the entropy contribution to the adsorption process.[47,48] On the contrary, the lower ΔD values found out for Gemini surfactant films points out that the entropy is the factor that controls the adsorption onto the sensor. To interpret this behavior, it is necessary to consider that fully extended hydrocarbon chains protrude to the liquid phase, resulting in high entropic contributions.[49] This seems to be the situation for the surfactant films, while the flatter configuration reached by the polymer molecules corresponds with lower entropic contribution to the variation of the adsorption free energy.[49]

We also carried out the study of the dynamic and thermodynamic properties of the polymer and surfactant films by analyzing the adsorption curves. These curves were registered introducing in the cell solutions of different coating concentrations ranging from 10^{-5} to 10^{-2} M. The surface concentration values, $\Gamma(t)$, were calculated from the frequency change (Δf) using the Sauerbrey model for surfactant films and the Voigt model for the polymer ones. The equilibrium surface concentration for each solution, Γ, was taken as the surface concentration at the saturation for each adsorption curve. Two representative examples of the variation of $\Gamma(t)$ with time for the polymer and surfactant molecules are presented in Figure 2s of the Supporting Information. Figure 3a and b shows the variation of the equilibrium surface concentration, Γ, with the polymer and surfactant concentration, respectively. As can be seen in Figure 3, the surface concentration increases with the polymer or surfactant concentration of solutions in the cell until it reaches a constant value referred as the maximum surfactant concentration adsorbed onto the sensor, Γ_{max}. From the curve morphology, it is possible to assume that the adsorption of PMAO and 18-2-18 onto the sensor could be interpreted by the Langmuir adsorption model. To confirm this assumption, the experimental values were fitted to the Langmuir equation:

$$\Gamma = \frac{\Gamma_{max} K_L C}{1 + K_L C} \tag{2}$$

In eq 2, K_L represents the Langmuir equilibrium constant and C is the solution concentration in the cell. Table 1 gathers the parameters obtained from the best fits. Lines in Figure 3 represent the Γ values calculated from eq 2 and the parameters in Table 1. The good agreement between experimental and calculated values indicates that the Langmuir model seems to interpret properly the adsorption of coatings onto the sensor.

From data in Table 1, one can conclude that the Langmuir equilibrium constant (K_L) is higher for the Gemini surfactant than for the polymer PMAO. Since K_L is defined by $K_L = k_a/k_d$, where k_a and k_d represent the constant rates of the adsorption and desorption processes, respectively, the K_L values found in this work indicate that the adsorption−desorption balance is more favorable for the Gemini surfactant than for the polymer

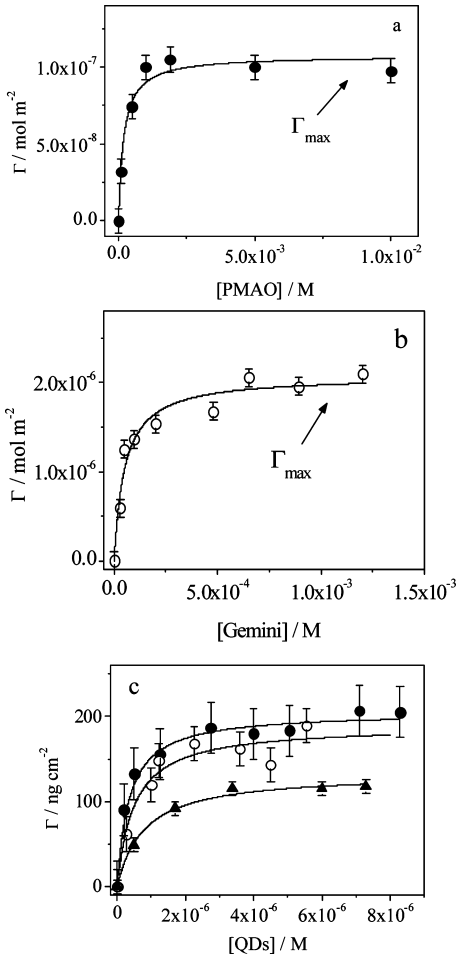

Figure 3. Adsorption isotherms of (a) PMAO and (b) Gemini surfactant adsorbed onto the sensor and (c) QDs onto PMAO (circles), Gemini surfactant (open circles), and on the bare sensor (triangles). The solid lines are calculated from eq 2 and parameters in Tables 1 and 2.

PMAO. On the other hand, the maximum surfactant concentration adsorbed onto the sensor (Γ_{max}) is more than 20 times the maximum polymer concentration. To interpret this behavior, it is necessary to consider that the interaction between the sensor (SiO_2) and the coatings is across the hydrophilic groups of the coating molecules and these groups are very different for the two molecules employed as coatings. According to the chemical structures of molecules, in the case of the Gemini surfactant, it is expected that the cationic headgroup was adsorbed on the oppositely charged sensor,[50] while interactions between the polymer PMAO and the sensor involves intermolecular interactions, likely across hydrogen bonding.[51] As a consequence, the attractions between oppositely charged groups are stronger than across the hydrogen bonds and drive to higher solid coverage.

The adsorption curves do not follow an exponential law (see Figure 3s of the Supporting Information) and can be interpreted as the sum of two exponential functions by[52]

$$\Gamma(t) = \Gamma - A_1 \exp(-t/\tau_1) - A_2 \exp(-t/\tau_2) \tag{3}$$

This means that the adsorption of both the polymer and surfactant molecules agrees with a bimodal process.[53,54] This is in agreement with the results obtained for the adsorption of several polymer molecules.[18,55−57] The characteristic time of

dx.doi.org/10.1021/la5024955 | Langmuir 2014, 30, 9977−9984

the two processes is almost independent of the concentration of the polymer or surfactant in the cell; see Figures 4s and 5s of the Supporting Information. The average value of τ_1 for the PMAO was (63 ± 28) s and for the Gemini surfactant (173 ± 50) s. These values are in the same order of magnitude as the adsorption times of polymer molecules;[56−58] therefore, we ascribed this time to the fast adsorption of surfactant and polymer molecules on the sensor surface. The slowest process presents characteristic times, τ_2, of (1415 ± 240) s for the polymer PMAO and (3180 ± 640) s for the Gemini surfactant. These values are quite similar to those ascribed to segment movements of polymer molecules adsorbed at the interfaces.[18,59]

According to our results, the adsorption of the polymer PMAO and the Gemini surfactant can be interpreted as follows: a first adsorption process, faster for the polymer than for the surfactant molecules, followed by rearrangements of the adsorbed molecules onto the sensor. From our data, it is possible to conclude that the rearrangement movements are slower in surfactant than in polymer molecules adsorbed onto the solid sensor. This behavior is consistent with other results found in this work. Thus, ΔD and thickness values indicated that the surfactant molecules in films are more packed than the polymer ones. Accordingly, the chain movements of the surfactant molecules in films can be hindered, and consequently, the relaxation time corresponding to these movements are slower for the surfactant than for the polymer molecules.

3.2. Properties of QDs Films Adsorbed onto Polymer and Gemini Surfactant Films. The next step was to study the thermodynamic and dynamic properties of QDs adsorbed onto polymer PMAO and the Gemini surfactant films by means of QCM-D. Figures 4 and 5 present typical records obtained at

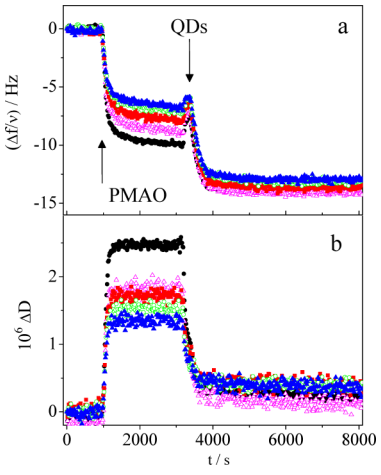

Figure 4. Time dependence of $\Delta f/\nu$ and ΔD shifts for different frequency overtones, 3rd (black), 5th (pink), 7th (red), 9th (green), and 11th (blue), during the absorption of QDs onto a PMAO film.

different frequency overtones for QDs adsorbed onto the polymer PMAO and the Gemini surfactant films, respectively. The first and second stages correspond to the baseline and the adsorption of the coatings, respectively. After the end of the coating adsorption, taken when $\Delta f/\nu$ and ΔD reach a constant value, the QD solutions were introduced in the cell and the frequency and dissipation changes were recorded until they reached constant values, steady state of the QD adsorption

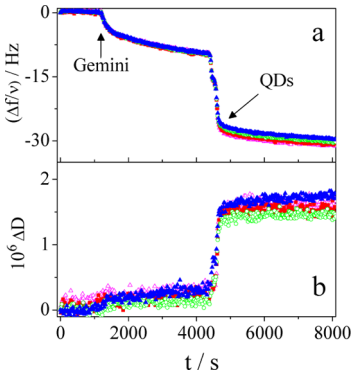

Figure 5. Time dependence of $\Delta f/\nu$ and ΔD shifts for different frequency overtones, 5th (pink), 7th (red), 9th (green), and 11th (blue), during the absorption of QDs onto a Gemini surfactant film..

process. The PMAO and the Gemini surfactant solutions chosen to build the first layer were 1×10^{-2} M (PMAO) and 1×10^{-3} M (Gemini surfactant). We choose these concentrations because, as was demonstrated above, the sensor is saturated with the coatings at these solution concentrations. For the sake of comparison, QDs were directly adsorbed onto the bare sensor, and changes in frequency and dissipation were recorded with time. An illustrative example is collected in Figure 6. From

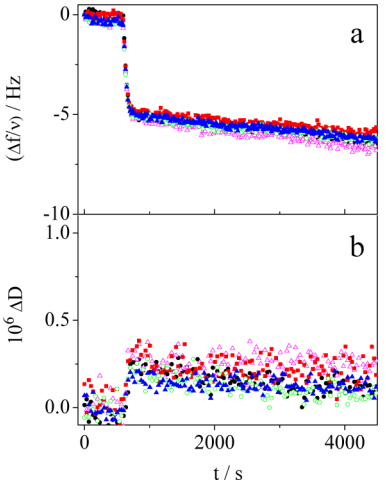

Figure 6. Time dependence of the $\Delta f/\nu$ and ΔD shifts for different frequency overtones, 3rd (black), 5th (pink), 7th (red), 9th (green), and 11th (blue), during the absorption of QDs onto the bare sensor.

results in Figures 4−6, it is possible to notice two different behaviors. The first one is observed for QDs deposited onto the bare sensor and on the Gemini surfactant film. As can be seen in Figures 5 and 6, the changes in frequency and dissipation for different overtones converge in master curves. This means that the QD films deposited directly onto the sensor and on the Gemini film present a rigid behavior.[42] In contrast, curves corresponding to QDs adsorbed onto the PMAO film show that, after the stage of polymer adsorption in which Δf and ΔD curves are characteristic of the viscoelastic system of PMAO films, the introduction of the QD solution in the cell decreases the ΔD value until it reaches a constant value (Figure 5). The constant ΔD values reached for the different overtones converge in a value. This fact indicates that the QD adsorption onto PMAO modifies the rheological properties of the polymer

dx.doi.org/10.1021/la5024955 | Langmuir 2014, 30, 9977−9984

film, and thus the viscous behavior of PMAO films disappears when nanoparticles are adsorbed on the polymer.

We use the adsorption curves to obtain information about the kinetic and the thermodynamic behavior of QDs adsorbed onto coating films. Figure 3c presents the variation of the QD equilibrium surface concentration values, Γ, with the QD concentration of solutions introduced in the cell. To determine the surface concentration, we use experimental Δf values and the Sauerbrey equation for all systems because QD films present elastic behavior. On the other hand, Γ is expressed in terms of QD mass because it was not possible to know the molecular weight of nanoparticles. The QD concentration of solutions introduced in the cell was determined from the UV−vis absorption spectrum of QDs dissolved in chloroform.[37] Results in Figure 3c show that the QD coverage increases significantly when nanoparticles are adsorbed onto the coating films compared with the bare sensor. The adsorption isotherms are interpreted according to the Langmuir model. Lines in Figure 3c represent the Γ values calculated from the Langmuir equation, eq 2, and the best-fit parameters collected in Table 2.

Table 2. K_L and Γ_{max} Values Obtained for the Fitting of the QD Absorption Data to the Langmuir Equation[a]

coating	K_L/(mol L)$^{-1}$	Γ_{max}/ng cm^{-2}	θ/g mol^{-1} chain
SiO_2	$(1.3 \pm 0.2) \times 10^6$	130 ± 5	
PMAO	$(3.6 \pm 0.6) \times 10^6$	200 ± 10	160 ± 10
Gemini	$(2.0 \pm 0.6) \times 10^6$	190 ± 15	450 ± 15

[a]The parameter θ represents the QDs coverage per hydrocarbon chain of coating, see text.

As can be seen in Figure 3c, the values calculated by eq 2 acceptably agree with the experimental data. From data in Table 2, it is possible to conclude that K_L and Γ_{max} almost duplicate their values when QDs are adsorbed onto PMAO or the Gemini films with respect to the adsorption onto the bare sensor. However, K_L and Γ_{max} do not depend significantly on the nature of the coating molecules. To understand the behavior of Γ_{max}, we analyze results in terms of QDs coverage per hydrocarbon chain, θ. The θ value was calculated as the ratio between the maximum surface concentration of QDs adsorbed onto films and the surface concentration of hydrocarbon chains. The latter was determined from Γ_{max} values determined in this work and taking into account that the polymer contains 114 hydrocarbon chains per molecule and the surfactant presents two hydrocarbon chains per molecule. The θ values found are collected in Table 2 and show that the QD coverage per hydrocarbon chain is almost three times higher for the Gemini surfactant than for the polymer PMAO. We relate this behavior to the different structure of molecules in films. Thus, since ΔD and thickness results indicate that the Gemini surfactant is perpendicular to the solid surface while PMAO lies flat to the sensor, it becomes clear that the surfactant configuration favors the contact between the hydrocarbon moieties of the QD stabilizer and the coating molecules, increasing the nanoparticle coverage per hydrocarbon chain unit.

Summarizing, our results seem to indicate that the adsorption of QDs on the coated sensor is a subtle balance between the coating ability to absorb QDs and the number of hydrocarbon chains per molecule of coatings. Thus, even though the surfactant configuration at the interface seems to be more advantageous to adsorb nanoparticles than that of the polymer, the higher number of hydrocarbon chains per polymer molecule compensates its lower ability of adsorbing nanoparticles. The result is QD coverage quite similar for both coatings.

To carry out the kinetic analysis of the QDs adsorption, we have chosen the adsorption curves corresponding to QDs solution concentrations above 2×10^{-6} M. This is to guarantee that the amount of QDs is enough to study properly the dynamics of the nanoparticle adsorption. The QD adsorption curves were interpreted by using the bimodal kinetic model of eq 3. The τ_1 and τ_2 values obtained in the fitting procedure are almost independent of both, the nature of the coating film and the concentration of QD solutions in the cell; see Figure 6s of the Supporting Information. Moreover, the characteristic times of the two processes, τ_1 and τ_2, present similar values for QDs adsorbed onto polymer and surfactant films and onto the bare sensor. This means that the kinetics of adsorption is driven by the QD adsorption, and does not depend on the coating employed. The average τ_1 and τ_2 values found in this work were (70 ± 40) s and (2500 ± 570) s, respectively. According to the magnitude of τ_1 and τ_2 values, the fastest process was ascribed to nanoparticle adsorption while the slowest one was assigned to rearrangement movements.[18,56,59,60] The latter agrees very well with the relaxation time value of rearrangements inside domains of CdSe QDs and poly(styrene-*co*-maleic anhydride) partial 2-butoxyethyl ester cumene terminated films.[18]

4. CONCLUSIONS

We employed the QCM-D technique to study the effect of two coatings, the polymer PMAO and the Gemini surfactant 18-2-18, on the coverage, the kinetics of adsorption, and the rheological properties of CdSe QD films. The results presented in this work demonstrated that these coatings improve the QD coverage and that the QD coverage per hydrocarbon chain of coating is higher for nanoparticles deposited on the Gemini surfactant than onto the polymer films. Our results point to the molecular conformation of the surfactant film as the main reason for this behavior. We also demonstrated that both the rheological properties of QD films adsorbed onto PMAO and onto Gemini surfactant and the kinetics of the adsorption of nanoparticles are independent of coatings and present similar values to those corresponding to QDs adsorbed onto the bare sensor. This means that these properties are driven by QDs. Finally, our results demonstrate that it is possible to increase the QD coverage on solids by modifying the nature of the molecules selected to coat the solid substrate.

■ ASSOCIATED CONTENT

Supporting Information

Rheological properties of PMAO films. Kinetic analysis of adsorption curves. This material is available free of charge via the Internet at http://pubs.acs.org.

■ AUTHOR INFORMATION

Corresponding Author

*Mailing Address: Departamento de Química Física, Facultad de Ciencias Químicas, Universidad de Salamanca, Plaza de los Caídos s/n, 37008 Salamanca, Spain. Fax: 00-34-923294500 Ext 1547. E-mail: mvsal@usal.es.

Notes

The authors declare no competing financial interest.

■ ACKNOWLEDGMENTS

The authors are thankful for financial support from ERDF and MEC (MAT 2010-19727). T.A. wishes to thank the European Social Fund and Consejería de Educación de la Junta de Castilla y León for her FPI grant.

■ REFERENCES

(1) Coe, S.; Woo, W. K.; Bawendi, M.; Bulovic, V. Electroluminescence from Single Monolayers of Nanocrystals in Molecular Organic Devices. *Nature* **2002**, *420*, 800.
(2) Talapin, D. V.; Lee, J.-S.; Kovalenko, M. V.; Shevchenko, E. V. Prospects of Colloidal Nanocrystals for Electronic and Optoelectronic Applications. *Chem. Rev.* **2010**, *110*, 389−458.
(3) Rogach, A. L. *Semiconductor Nanocrystal Quantum Dots: Synthesis, Assembly, Spectroscopy and Applications*; Springer: Wien, New York, 2008.
(4) Zhou, J.; Li, H. Highly Fluorescent Fluoride-Responsive Hydrogels Embedded with CdTe Quantum Dots. *ACS Appl. Mater. Interfaces* **2012**, *4*, 721−724.
(5) Zhou, J.; Huang, J.; Tian, D.; Li, H. Cyclodextrin Modified Quantum Dots with Tunable Liquid-Like Behaviour. *Chem. Commun.* **2012**, *48*, 3596−3598.
(6) Wang, J.; Vennerberg, D.; Lin, Z. Quantum Dot Sensitized Solar Cells. *J. Nanoeng. Nanomanuf.* **2011**, *1*, 155−171.
(7) Talapin, D. V.; Murray, C. B. PbSe Nanocrystal Solids for n- and p-Channel Thin Film Field-Effect Transistors. *Science* **2005**, *310*, 86−89.
(8) Bigioni, T. P.; Lin, X.-M.; Nguyen, T. T.; Corwin, E. I.; Witten, T. A.; Jaeger, H. M. Kinetically Driven Self Assembly of Highly Ordered Nanoparticle Monolayers. *Nat. Mater.* **2006**, *5*, 265−270.
(9) Baker, J. L.; Widmer-Cooper, A.; Toney, M. F.; Geissler, P. L.; Alivisatos, A. P. Device-Scale Perpendicular Alignment of Colloidal Nanorods. *Nano Lett.* **2010**, *10*, 195−201.
(10) Gao, Y.; Tang, Z. Design and Application of Inorganic Nanoparticle Superstructures: Current Status and Future Challenges. *Small* **2011**, *7*, 2133−2146.
(11) Sear, R. P.; Chung, S.-W.; Markovich, G.; Gelbart, W. M.; Heath, J. R. Spontaneous Patterning of Quantum Dots at the Air-Water Interface. *Phys. Rev. E* **1999**, *59*, R6255−R6258.
(12) Ganesan, V. Some Issues in Polymer Nanocomposites: Theoretical and Modeling Opportunities for Polymer Physics. *J. Polym. Sci., Part B: Polym. Phys.* **2008**, *46*, 2666−2671.
(13) Bockstaller, M. R.; Thomas, E. L. Optical Properties of Polymer-Based Photonic Nanocomposite Materials. *J. Phys. Chem. B* **2003**, *107*, 10017−10024.
(14) Alejo, T.; Martín-García, B.; Merchán, M. D.; Velázquez, M. M. QDs Supported on Langmuir-Blodgett Films of Polymers and Gemini Surfactant. *J. Nanomater.* **2013**, *2013*, 10.
(15) Alejo, T.; Merchán, M. D.; Velázquez, M. M.; Pérez-Hernández, J. A. Polymer/Surfactant Assisted Self-Assembly of Nanoparticles into Langmuir−Blodgett Films. *Mater. Chem. Phys.* **2013**, *138*, 286−294.
(16) Martín-García, B.; Velázquez, M. M. Block Copolymer Assisted Self-Assembly of Nanoparticles into Langmuir−Blodgett Films: Effect of Polymer Concentration. *Mater. Chem. Phys.* **2013**, *141*, 324−332.
(17) Martín-García, B.; Paulo, P. M. R.; Costa, S. M. B.; Velázquez, M. M. Photoluminescence Dynamics of CdSe QD/Polymer Langmuir−Blodgett Thin Films: Morphology Effects. *J. Phys. Chem. C* **2013**, *117*, 14787−14795.
(18) Martín-García, B.; Velázquez, M. M. Nanoparticle Self-Assembly Assisted by Polymers: The Role of Shear Stress in the Nanoparticle Arrangement of Langmuir and Langmuir−Blodgett Films. *Langmuir* **2013**, *30*, 509−516.
(19) Liu, M.; Gan, L.; Zeng, Y.; Xu, Z.; Hao, Z.; Chen, L. Self-Assembly of CdTe Nanocrystals into Two-Dimensional Nanoarchitectures at the Air−Liquid Interface Induced by Gemini Surfactant of 1,3-Bis(hexadecyldimethylammonium) Propane Dibromide. *J. Phys. Chem. C* **2008**, *112*, 6689−6694.
(20) Petty, M. C. *Langmuir−Blodgett Films: An Introduction*; Cambridge University Press: Cambridge, 1996.
(21) Zhavnerko, G.; Marletta, G. Developing Langmuir−Blodgett Strategies Towards Practical Devices. *Mater. Sci. Eng., B* **2010**, *169*, 43−48.
(22) Bronstein, L. M.; Shtykova, E. V.; Malyutin, A.; Dyke, J. C.; Gunn, E.; Gao, X.; Stein, B.; Konarev, P. V.; Dragnea, B.; Svergun, D. I. Hydrophilization of Magnetic Nanoparticles with Modified Alternating Copolymers. Part 1: The Influence of the Grafting. *J. Phys. Chem. C* **2010**, *114*, 21900−21907.
(23) Shtykova, E. V.; Huang, X.; Gao, X.; Dyke, J. C.; Schmucker, A. L.; Dragnea, B.; Remmes, N.; Baxter, D. V.; Stein, B.; Konarev, P. V.; Svergun, D. I.; Bronstein, L. M. Hydrophilic Monodisperse Magnetic Nanoparticles Protected by an Amphiphilic Alternating Copolymer. *J. Phys. Chem. C* **2008**, *112*, 16809−16817.
(24) Yu, W. W.; Chang, E.; Sayes, C. M.; Drezek, R.; Colvin, V. L. Aqueous Dispersion of Monodisperse Magnetic Iron Oxide Nanocrystals through Phase Transfer. *Nanotechnology* **2006**, *17*, 4483.
(25) Pellegrino, T.; Manna, L.; Kudera, S.; Liedl, T.; Koktysh, D.; Rogach, A. L.; Keller, S.; RÃ¤dler, J.; Natile, G.; Parak, W. J. Hydrophobic Nanocrystals Coated with an Amphiphilic Polymer Shell: A General Route to Water Soluble Nanocrystals. *Nano Lett.* **2004**, *4*, 703−707.
(26) Jin, J.; Li, L. S.; Tian, Y. Q.; Zhang, Y. J.; Liu, Y.; Zhao, Y. Y.; Shi, T. S.; Li, T. J. Structure and Characterization of Surfactant-Capped CdS Nanoparticle Films by the Langmuir−Blodgett Technique. *Thin Solid Films* **1998**, *327-329*, 559−562.
(27) Chen, X.; Wang, J.; Shen, N.; Luo, Y.; Li, L.; Liu, M.; Thomas, R. K. Gemini Surfactant/DNA Complex Monolayers at the Air−Water Interface: Effect of Surfactant Structure on the Assembly, Stability, and Topography of Monolayers. *Langmuir* **2002**, *18*, 6222−6228.
(28) Chen, Q.; Kang, X.; Li, R.; Du, X.; Shang, Y.; Liu, H.; Hu, Y. Structure of the Complex Monolayer of Gemini Surfactant and DNA at the Air/Water Interface. *Langmuir* **2012**, *28*, 3429−3438.
(29) Coe, S.; Woo, W.-K.; Bawendi, M.; Bulovic, V. Electroluminescence from Single Monolayers of Nanocrystals in Molecular Organic Devices. *Nature* **2002**, *420*, 800−803.
(30) Saunders, B. R. Hybrid Polymer/Nanoparticle Solar Cells: Preparation, Principles and Challenges. *J. Colloid Interface Sci.* **2012**, *369*, 1−15.
(31) Gole, A.; Jana, N. R.; Selvan, S. T.; Ying, J. Y. Langmuir−Blodgett Thin Films of Quantum Dots: Synthesis, Surface Modification, and Fluorescence Resonance Energy Transfer (FRET) Studies. *Langmuir* **2008**, *24*, 8181−8186.
(32) Park, J. J.; Lacerda, S. H. D. P.; Stanley, S. K.; Vogel, B. M.; Kim, S.; Douglas, J. F.; Raghavan, D.; Karim, A. Langmuir Adsorption Study of the Interaction of CdSe/ZnS Quantum Dots with Model Substrates: Influence of Substrate Surface Chemistry and pH. *Langmuir* **2009**, *25*, 443−450.
(33) Alcantara, G. B.; Paterno, L. G.; Afonso, A. S.; Faria, R. C.; Pereira-da-Silva, M. A.; Morais, P. C.; Soler, M. A. G. Adsorption of Cobalt Ferrite Nanoparticles within Layer-by-Layer Films: A Kinetic Study Carried out Using Quartz Crystal Microbalance. *Phys. Chem. Chem. Phys.* **2011**, *13*, 21233−21242.
(34) Zana, R.; Benrraou, M.; Rueff, R. Alkanediyl-α,Ω-bis-(dimethylalkylammonium bromide) Surfactants. 1. Effect of the Spacer Chain Length on the Critical Micelle Concentration and Micelle Ionization degree. *Langmuir* **1991**, *7*, 1072−1075.
(35) Alejo, T.; Merchán, M. D.; Velázquez, M. M. Specific Ion Effects on the Properties of Cationic Gemini Surfactant Monolayers. *Thin Solid Films* **2011**, *519*, 5689−5695.
(36) Yu, W. W.; Peng, X. Formation of High-Quality CdS and Other II−VI Semiconductor Nanocrystals in Noncoordinating Solvents: Tunable Reactivity of Monomers. *Angew. Chem., Int. Ed. Engl.* **2002**, *41*, 2368−2371.
(37) Jasieniak, J.; Smith, L.; Embden, J. v.; Mulvaney, P.; Califano, M. Re-examination of the Size-Dependent Absorption Properties of CdSe Quantum Dots. *J. Phys. Chem. C* **2009**, *113*, 19468−19474.

(38) Höök, F.; Kasemo, B.; Nylander, T.; Fant, C.; Sott, K.; Elwing, H. Variations in Coupled Water, Viscoelastic Properties, and Film Thickness of a Mefp-1 Protein Film during Adsorption and Cross-Linking: A Quartz Crystal Microbalance with Dissipation Monitoring, Ellipsometry, and Surface Plasmon Resonance Study. *Anal. Chem.* **2001**, *73*, 5796−5804.
(39) Sauerbrey, G. Verwendung von Schwingquarzen zur Wägung dünner Schichten und zur Mikrowägung. *Z. Phys.* **1959**, *155*, 206−222.
(40) Voinova, M. V.; Rodahl, M.; Jonson, M.; Kasemo, B. Viscoelastic Acoustic Response of Layered Polymer Films at Fluid-Solid Interfaces: Continuum Mechanics Approach. *Phys. Scr.* **1999**, *59*, 391.
(41) Steinem, C.; Janshoff, A. *Piezoelectric Sensors*; Springer-Verlag: Berlin, 2007.
(42) Benedetti, T. M.; Torresi, R. M. Rheological Changes and Kinetics of Water Uptake by Poly(ionic liquid)-Based Thin Films. *Langmuir* **2013**, *29*, 15589−15595.
(43) Nejadnik, M. R.; Olsson, A. L. J.; Sharma, P. K.; van der Mei, H. C.; Norde, W.; Busscher, H. J. Adsorption of Pluronic F-127 on Surfaces with Different Hydrophobicities Probed by Quartz Crystal Microbalance with Dissipation. *Langmuir* **2009**, *25*, 6245−6249.
(44) Irwin, E. F.; Ho, J. E.; Kane, S. R.; Healy, K. E. Analysis of Interpenetrating Polymer Networks via Quartz Crystal Microbalance with Dissipation Monitoring. *Langmuir* **2005**, *21*, 5529−5536.
(45) Gurdak, E.; Dupont-Gillain, C. C.; Booth, J.; Roberts, C. J.; Rouxhet, P. G. Resolution of the Vertical and Horizontal Heterogeneity of Adsorbed Collagen Layers by Combination of QCM-D and AFM. *Langmuir* **2005**, *21*, 10684−10692.
(46) Höök, F.; Rodahl, M.; Brzezinski, P.; Kasemo, B. Energy Dissipation Kinetics for Protein and Antibody−Antigen Adsorption under Shear Oscillation on a Quartz Crystal Microbalance. *Langmuir* **1998**, *14*, 729−734.
(47) Olanya, G.; Iruthayaraj, J.; Poptoshev, E.; Makuska, R.; Vareikis, A.; Claesson, P. M. Adsorption Characteristics of Bottle-Brush Polymers on Silica: Effect of Side Chain and Charge Density. *Langmuir* **2008**, *24*, 5341−5349.
(48) Ozeki, T.; Morita, M.; Yoshimine, H.; Furusawa, H.; Okahata, Y. Hydration and Energy Dissipation Measurements of Biomolecules on a Piezoelectric Quartz Oscillator by Admittance Analyses. *Anal. Chem.* **2006**, *79*, 79−88.
(49) Tandford, C. *The Hydrofobic Effect: Formation of Micelles and Biological Membranes*; Wiley-Interscience: New York, 1980, p 22.
(50) Esumi, K.; Matoba, M.; Yamanaka, Y. Characterization of Adsorption of Quaternary Ammonium Cationic Surfactants and Their Adsolubilization Behaviors on Silica. *Langmuir* **1996**, *12*, 2130−2135.
(51) Lin, H.-P.; Mou, C.-Y. Structural and Morphological Control of Cationic Surfactant-Templated Mesoporous Silica. *Acc. Chem. Res.* **2002**, *35*, 927−935.
(52) Raposo, M.; Pontes, R. S.; Mattoso, L. H. C.; Oliveira, O. N. Kinetics of Adsorption of Poly(o-methoxyaniline) Self-Assembled Films. *Macromolecules* **1997**, *30*, 6095−6101.
(53) Chiang, C.-Y.; Starov, V. M.; Lloyd, D. R. Crystallization Kinetics of a Polymer-Solvent System. I: Derivation of Model Equations. *Colloid J.* **1995**, *57*, 715−724.
(54) Chiang, C. Y.; Starov, V. M.; Hall, M. S.; Lloyd, D. R. Crystallization Kinetics of Polymer-Solvent Systems: 2. Experimental Verification of the Model. *Colloid J.* **1997**, *59*, 236−247.
(55) Guzmán, E.; Ortega, F.; Baghdadli, N.; Luengo, G. S.; Rubio, R. G. Effect of the Molecular Structure on the Adsorption of Conditioning Polyelectrolytes on Solid Substrates. *Colloids Surf., A* **2011**, *375*, 209−218.
(56) Guzmán, E.; Ritacco, H.; Ortega, F.; Rubio, R. G. Evidence of the Influence of Adsorption Kinetics on the Internal Reorganization of Polyelectrolyte Multilayers. *Colloids Surf., A* **2011**, *384*, 274−281.
(57) Guzmán, E.; Cavallo, J. A.; Chuliá-Jordán, R.; Gómez, C. s.; Strumia, M. C.; Ortega, F.; Rubio, R. n. G. pH-Induced Changes in the Fabrication of Multilayers of Poly(acrylic acid) and Chitosan: Fabrication, Properties, and Tests as a Drug Storage and Delivery System. *Langmuir* **2011**, *27*, 6836−6845.
(58) Guzmán, E.; Ritacco, H. n.; Ortega, F.; Svitova, T.; Radke, C. J.; Rubio, R. n. G. Adsorption Kinetics and Mechanical Properties of Ultrathin Polyelectrolyte Multilayers: Liquid-Supported versus Solid-Supported Films. *J. Phys. Chem. B* **2009**, *113*, 7128−7137.
(59) Muñoz, M. G.; Monroy, F.; Ortega, F.; Rubio, R. G.; Langevin, D. Monolayers of Symmetric Triblock Copolymers at the Air−Water Interface. 2. Adsorption Kinetics. *Langmuir* **1999**, *16*, 1094−1101.
(60) Guzmán, E.; Ritacco, H. A.; Ortega, F.; Rubio, R. G. Growth of Polyelectrolyte Layers Formed by Poly(4-styrenesulfonate sodium salt) and Two Different Polycations: New Insights from Study of Adsorption Kinetics. *J. Phys. Chem. C* **2012**, *116*, 15474−15483.